Hindawi
Shock and Vibration
Volume 2020, Article ID 8812424, 14 pages
https://doi.org/10.1155/2020/8812424

Research Article

Influence of 3D Urban Dense Building Groups on Magnification of Ground Motion in Homogeneous Sedimentary Basin

Ping-Lin Jiang, Hua Jiang, Tian-Yi Yu, Tian-Yu Sun, and Lei Zhang

School of Mechanics and Civil Engineering, China University of Mining & Technology, Beijing 100083, China

Correspondence should be addressed to Hua Jiang; alandavidrain@163.com

Received 30 April 2020; Revised 8 July 2020; Accepted 18 July 2020; Published 30 August 2020

Academic Editor: Francisco Beltran-Carbajal

By using the harmonic response analysis in the finite element analysis method, the seismic dynamic interaction of the three-dimensional urban building group-homogeneous sedimentary basin is studied. The viscoelastic artificial boundary is introduced, which can overcome both the defects of low-frequency drift and high-frequency instability, and the equivalent load in frequency domain is obtained by fast Fourier transform for loading, to explore the influence of the different incident frequencies (0.5–5.0 Hz), different numbers (196, 400, 676), and spacing (55 m, 62.5 m, 70 m) of building groups on the ground motion of homogeneous sedimentary basin under the incidence of SV wave. Numerical results illustrate that at low frequency, the displacement cloud image of the homogeneous sedimentary basin model shows an obvious phenomenon of "central focusing." With the increase of frequency, the displacement cloud image gradually changes from "central focusing" to "multipoint focusing." Meanwhile, the displacement peak gradually moves from the surface to the center of the basin. At a certain incident frequency, the existence of dense building groups will change the spatial distribution of displacement amplitude in the basin. Under the action of high-frequency incident waves, denser building groups with more buildings and smaller building spacing have a more pronounced weakening effect on the seismic response of homogeneous sedimentary basins. The displacement response of the center of the basin is generally large. When planning important buildings, the center area should be avoided as much as possible. For existing buildings, structural reinforcement is needed. It is of great significance for the planning and layout of buildings in the soft sedimentary basin and the reasonable spacing of buildings to reduce the risk of urban earthquake disaster.

1. Introduction

Site-City Interaction (SCI) under seismic wave incidence is an active research topic in many fields such as the geotechnical engineering, earthquake engineering, and geophysics. In recent years, with the acceleration of urbanization, buildings become more and dense, making the scale of "Site-Building Groups" larger and larger, which brings new challenges to the seismic safety assessment of the existing buildings on the site and the seismic fortification of the proposed project. In general, the analysis methods of site-city interaction can be divided into the analytical method and numerical method. Analytic solutions usually refer to the wave function expansion method [1–5], the complex variable method [6,7], etc. Numerical solutions mainly include finite element method [8–11], finite difference method [12–14], boundary element method [15–17], discrete wave number method [18], and hybrid method [19,20].

As a special site, the significant amplification effect of the sedimentary basin on ground motion has been confirmed by a large number of examples of earthquake damage [20–23]. In terms of theoretical research, Trifunac [24] and Lee [25], respectively, solved the two-dimensional scattering problem of incident plane SH waves in a semicylindrical alluvial valley and the analytical solution of incident plane waves in a three-dimensional hemispherical depression topography by using the wave function expansion method. Li et al. [26] used the finite difference method to study the site amplification effect of the octave earthquake anomaly area in Hanyuan County during the 2008 Wenchuan earthquake and concluded that the valley topography had a significant impact on the ground motion.

However, the presence of buildings/groups will have a significant impact on the site effect, and many experts and scholars have carried out a lot of research on this. Wirgin and Bard [27] studied the resonance law between the soil layer and a large number of buildings by establishing a two-dimensional "SCI" numerical model and explained some special seismic damage phenomena in the Mexico earthquake (1985). Clouteau and Aubry [28] analyzed the influence of the distribution of building groups on the ground motion characteristics and structural response based on the three-dimensional boundary element method. Tsogka and Wirgin [29] used the finite element method to study the "SCI" problem of soft soil-building groups (homogeneous block model) under SH wave excitation, and the results showed that the seismic response of building groups showed great heterogeneity due to multiple coherent effects of seismic waves. Kham et al. [30] used the two-dimensional boundary element method to analyze the influence of factors such as spatial distribution and natural frequency of urban buildings under the incidence of SH wave and found that the "SCI" effect was most obvious when the frequencies of buildings and foundations were the same. Taborda and Bielak [31] found that the existence of building groups significantly affected the seismic response in and around the city. Using the periodic green function, Volkov and Zheltukhin [32] proposed an efficient method to study the interaction between building groups and the overall resonance effect. He et al. [33] used the wave finite element method to establish a two-dimensional model of buildings and sedimentary valley. By comparing the seismic responses in frequency domain and time domain of individual sedimentary valley and building groups and sedimentary valley, they found that the existence of building groups has a significant impact on the seismic response of the valley.

It is worth noting that the above studies mainly focus on the single two-dimensional or three-dimensional site effect, as well as the dynamic interaction between the site and several buildings, and there is a lack of research on the dynamic interaction between the three-dimensional site-building groups. This paper uses the viscoelastic boundary wave finite element simulation method, build up to 676 buildings 3D building groups-homogeneous sedimentary basin model, and harmonic response analysis is introduced into solving the frequency domain solution, and explores the effects of the number and spacing of urban dense building groups on the ground motion of homogeneous sedimentary basins, so as to provide the theory basis for seismic fortification, etc.

2. Calculation Model

As shown in Figure 1, a three-dimensional dense building groups-homogeneous sedimentary basin model. In which, 1(a) is the homogeneous sedimentary basin with no buildings and 1(b) is building groups-homogeneous sedimentary basin model. Among them, the 8-node solid element and 10-node high-order solid element are selected for the soil, and the 8-node solid element is selected for the foundation. The three-dimensional beam element is used for the simulation of the building part. The building dynamic model adopts the equivalent concentrated mass rod model and by controlling the single particle system model to be the same as the first-order natural vibration period of the building to achieve the purpose of equivalent simplification. The foundation is directly coupled with the soil contacting part. Due to the symmetry of the calculation model, a 1/4 model is taken in the frequency domain to improve the calculation efficiency.

3. Viscoelastic Boundary and Ground Motion Input Method

3.1. Viscoelastic Boundary. In the simulation of soil boundary, in order to eliminate the reflection of waves on the truncated boundary and reduce the computational freedom, the viscoelastic boundary is used to treat the boundary of local foundation, as shown in Figure 2. Compared with viscous boundary [34] and transmission boundary [35], the viscoelastic boundary is an effective and suitable for solving complex seismic wave problems of artificial boundary [36]; it overcomes the low frequency drift problems caused by the viscous boundary, to simulate the artificial boundary outside the elastic recovery of semi-infinite medium performance, low-frequency and high-frequency stability is good, and easy to use.

In Figure 2, K_{BN}, K_{BT} are, respectively, the radial spring stiffness coefficient and tangential spring stiffness coefficient of viscoelastic boundary and C_{BN}, C_{BT}, respectively, are the radial spring damping coefficient and tangential spring damping coefficient of viscoelastic boundary. Among them,

$$\begin{aligned} K_{BN} &= \alpha_N \frac{G}{R_d}, \\ K_{BT} &= \alpha_T \frac{G}{R_d}, \\ C_{BN} &= \rho_0 v_p, \\ C_{BT} &= \rho_0 v_S, \end{aligned} \tag{1}$$

where G is the shear modulus of foundation, R is the distance between the scattered wave source and the artificial boundary, ρ_0 is the mass density of foundation, v_P is the compression wave velocity of soil, and v_S is the shear wave velocity of soil. In this article, $\alpha_N = 1.33$ and $\alpha_T = 0.67$.

3.2. Ground Motion Input Method. From the stress relationship at the viscoelastic boundary of the truncated soil mass, the equivalent nodal force formula on the viscoelastic artificial boundary can be obtained:

$$F_b(t) = \left(Ku + C\dot{u} + \sigma_b(t)\right) \cdot A_b, \tag{2}$$

where K is the stiffness coefficient matrix of the elastic element in the viscoelastic boundary and C is the damping coefficient matrix of the damper in the viscoelastic boundary. SV wave is incident from the top of bedrock, and

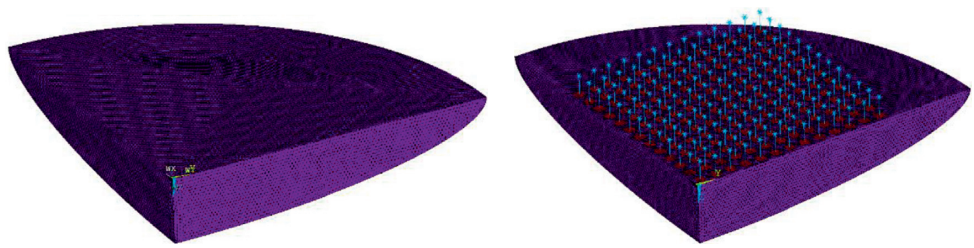

(a) (b)

Figure 1: The model of 3D dense building groups-homogeneous sedimentary basin: (a) no building; (b) building groups.

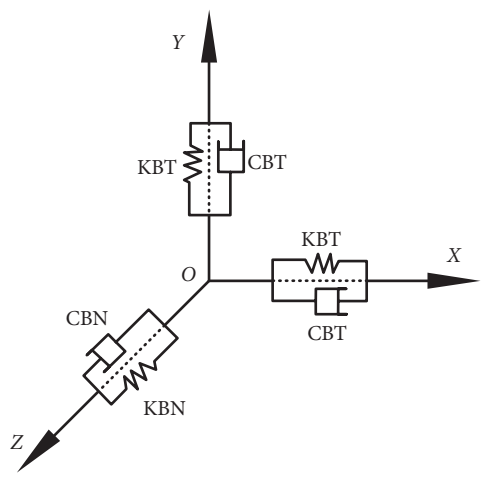

Figure 2: Viscoelastic boundary diagram.

its displacement u and acceleration $\dot{u}$ can be calculated according to one-dimensional wave theory, in which $\sigma_b(t)$ is the stress at the corresponding node on the viscoelastic boundary of the truncated soil in the free field and A_b is the influence area of each node on the viscoelastic artificial boundary. The equivalent load expressions (3)–(5) in the time domain can be obtained from the calculation and derivation of geometric equation and constitutive equation:

$$\begin{cases} F_x^{-x} = \left\{K_{BT}\left[u_0\left(t-\dfrac{h_d}{v_s}\right)+u_0\left(t-\dfrac{2H-h_d}{v_s}\right)\right]+C_{BT}\left[\dot{u}_0(t)+\dot{u}_0\left(t-\dfrac{2H-h_d}{v_s}\right)\right]\right\}\cdot A_b, \\ F_y^{-x} = 0, \\ F_z^{-x} = 0, \end{cases} \tag{3}$$

$$\begin{cases} F_x^{-y} = \left\{K_{BN}\left[u_0\left(t-\dfrac{h_d}{v_s}\right)+u_0\left(t-\dfrac{2H-h_d}{v_s}\right)\right]+C_{BN}\left[\dot{u}_0(t)+\dot{u}_0\left(t-\dfrac{2H-h_d}{v_s}\right)\right]\right\}\cdot A_b, \\ F_y^{-y} = 0, \\ F_z^{-y} = \rho c_s\left[\dot{u}_0(t)-\dot{u}_0\left(t-\dfrac{2H}{c_s}\right)\right], \end{cases} \tag{4}$$

$$\begin{cases} F_x^{-z} = \left\{K_{BT}\left[u_0(t)+u_0\left(t-\dfrac{2H}{v_s}\right)\right]+C_{BT}\left[\dot{u}_0(t)+\dot{u}_0\left(t-\dfrac{2H-h_d}{v_s}\right)\right]+\rho c_s\left[\dot{u}_0(t)-\dot{u}_0\left(t-\dfrac{2H}{c_s}\right)\right]\right\}\cdot A_b, \\ F_y^{-z} = 0, \\ F_z^{-z} = 0, \end{cases} \tag{5}$$

where the superscript of the equivalent load F represents the normal direction of the truncated boundary plane where the node is located and the subscript represents the equivalent load direction, ρ is the soil density, c_s is the shear wave velocity, H is the distance from the bottom boundary to the surface, and h_d is the distance from the node to the boundary on the artificial boundary.

As the number of elements of the 3D model in this paper reaches 10^6, the harmonic response analysis solution module is used to conduct frequency domain analysis of the site. First, the equivalent load in the time domain is converted to the equivalent load in the frequency domain by fast Fourier transform, and then the load is loaded for solution. The equivalent load on each viscoelastic boundary in the frequency domain is as follows:

$$\begin{cases} F_x^{-x} = \left[K_{BN} \cdot 2\cos(kz) + iC_{BN} \cdot 2\omega\cos(kz)\right] \cdot A_b, \\ F_y^{-x} = 0, \\ F_z^{-x} = \rho c_s \cdot (-1) \cdot 2\omega\sin(kz) \cdot A_b, \end{cases}$$
$$\begin{cases} F_x^{-y} = \left[K_{BT} \cdot 2\cos(kz) + iC_{BT} \cdot 2\omega\cos(kz)\right] \cdot A_b, \\ F_y^{-y} = 0, \\ F_z^{-y} = 0, \end{cases} \tag{6}$$
$$\begin{cases} F_x^{-z} = \left[K_{BT} \cdot 2\cos(kz) + \rho c_s \cdot (-1) \cdot 2\omega\sin(kz) \right. \\ \qquad \left. + iC_{BT} \cdot 2\omega\cos(kz)\right] \cdot A_b, \\ F_y^{-z} = 0, \\ F_z^{-z} = 0, \end{cases}$$

where ω is the circular frequency of the incident wave, k is the SV wave number, and z is the depth of the node (the distance from the surface).

4. Boundary Stability Verification and Accuracy Verification

4.1. Boundary Stability Verification. In order to test the correctness and stability of viscoelastic boundary, the truncation range of soil was selected as $2Ra$, $3Ra$, and $4Ra$ for comparative analysis and the sedimentary basin radius $Ra = 1000$ m. The higher dimensionless frequency $\eta = 2a/\lambda = \omega a/\pi c_s = 2.0$ are used in the free field verification to reflect the good applicability of viscoelastic boundary. The model parameters are shown in Table 1, and the simple harmonic SV wave is incident vertically from the bottom, and the incident amplitude is 1.

The x-direction displacement amplitude of the surface node on the x and y axes of the free field is shown in Figure 3. When the boundary dimensions are $2Ra$, $3Ra$, and $4Ra$, the maximum displacement in the x-direction of the surface node on the x-axis is 2.08904, 2.016, and 2.05671, and the minimum value is 1.93878, 1.91517, and 1.99879, respectively. The maximum displacement in the x-direction of the surface node on the y-axis is 2.08373, 2.00932, and 2.02299, and the minimum value is 1.99496, 1.92641, and 1.96558, respectively.

Figure 4 is the scatter diagram of the error analysis of the displacement amplitude and theoretical value of the ground node in the x direction on the x and y axes of the free field. Similar to the law of fixed boundary, the error between the simulation result and the theoretical value decreases with the increase of the model size. The three cases all meet the accuracy requirements within 5% of the engineering error. Considering the calculation accuracy and efficiency comprehensively, this paper selects $3Ra$ for the truncated soil area for the next numerical simulation analysis.

Table 1: List of some important notations and values of site.

Symbol	Description	Value
ρ	Soil density	2100 kg/m^3
v_s	Site shear wave velocity	1000 m/s
v_p	Site compression wave velocity	2000 m/s
ξ	Site damping ratio	0.03
ν	Site Poisson's ratio	1/3
G	Site shear modulus	2.1×10^9 Pa
E	Site elastic modulus	5.6×10^9 Pa

4.2. Accuracy Verification. In order to test the applicability of using viscoelastic boundary to solve the seismic response of sedimentary basins, the results of finite element simulation of viscoelastic boundary wave are compared with the theoretical results in [37]. Take the hemispherical sedimentary basin as the verification object; the model parameters are shown in Table 2; the incident wave is the SV wave with amplitude of 1. The results are shown in Figure 5.

It can be seen that the method in this paper is suitable for solving the seismic response of sedimentary basins. At the same time, the results in the figure also show that the presence of sedimentary basins has a more obvious amplification effect on seismic waves, and the further the basin center, the more significant the amplification effect, and the amplification effect in the main displacement direction of the basin center reaches 6 times. The focusing effect of sedimentary basin on incident wave is very significant.

5. Numerical Analysis

5.1. Site and Building Models. The simple point dynamic system is used to replace the building to simplify the modeling and reduce the calculation. The period of the dynamic system is the same as that of the building so as to achieve the dynamic equivalence of the structure. The single building is 64 m in height, and D is the spacing between buildings. The length and width of the foundation are 30 m, the height is 7.5 m, and the total mass is 2.21×10^7 kg. For the sedimentary basin, the radius R is 1000 m and the depth of the basin is 200 m. Other model parameters of the site and buildings are shown in Table 3. Take the dimensionless displacement and the incident wave amplitude is 1.0, and compare the magnification to discuss the amplification effect of the basin.

5.2. The Influence of Building Quantity on the Amplification Effect of Ground Motion in Homogeneous Sedimentary Basin. By comparing the displacement amplitude of the homogeneous sedimentary basin with different number of

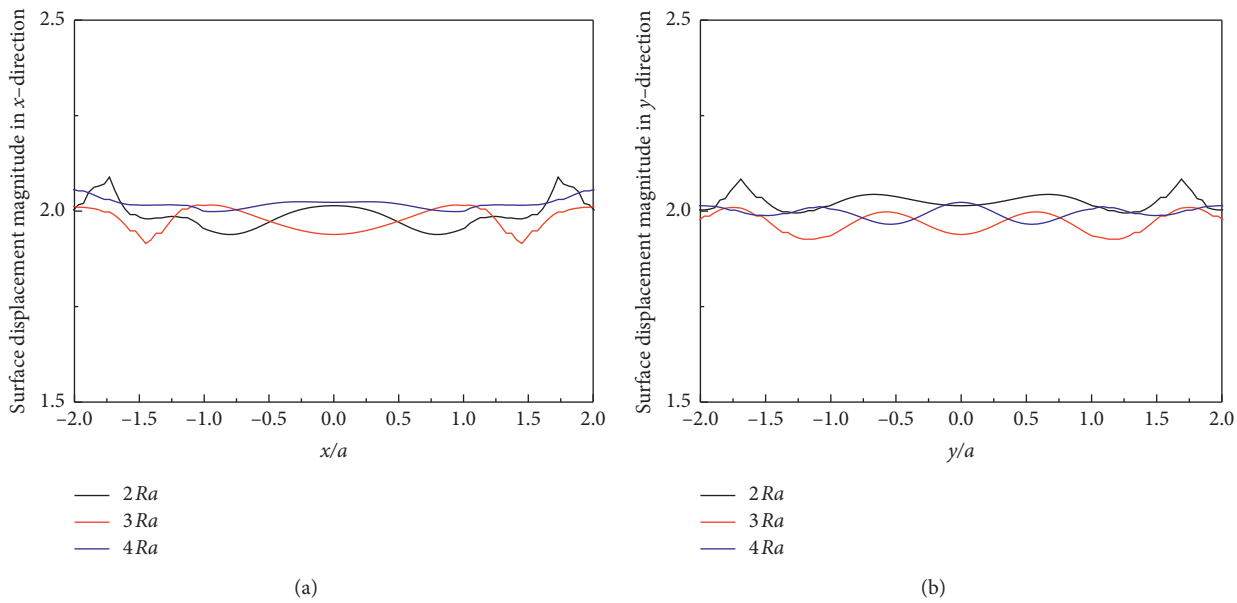

Figure 3: The x-direction displacement amplitude of the surface node of the free field: (a) the x-axis; (b) the y-axis.

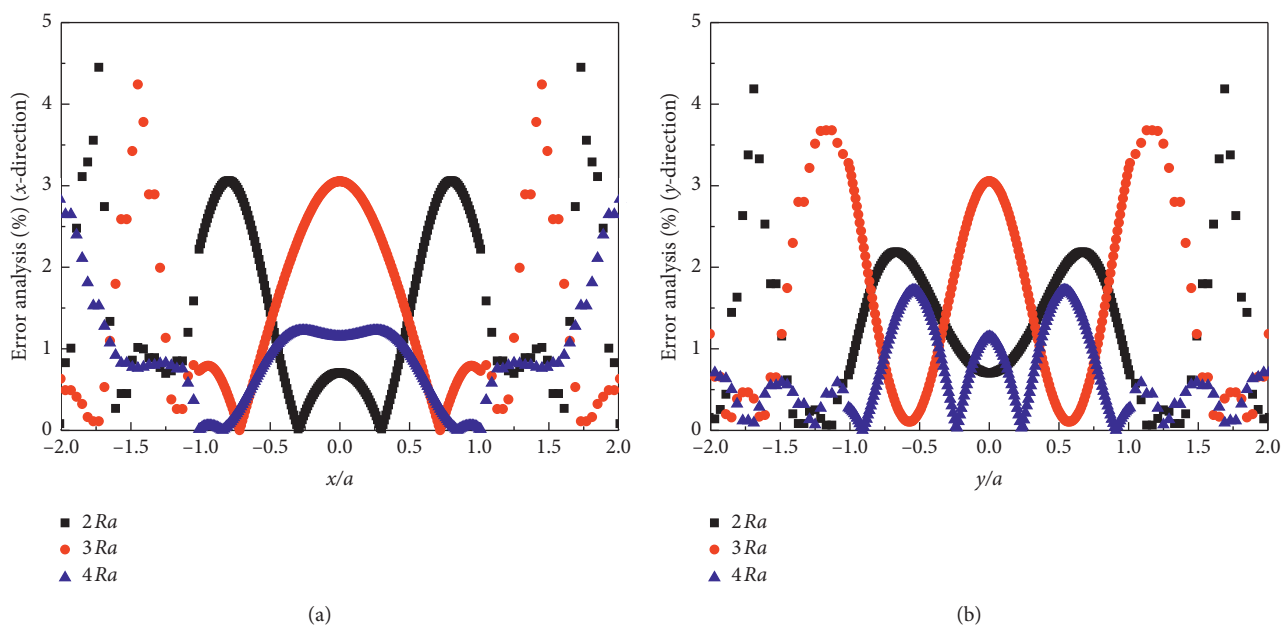

Figure 4: The error analysis diagram of the x-direction displacement amplitude and the theoretical value of the free field surface node: (a) the x-axis; (b) the y-axis.

Table 2: List of some important notations and values.

Symbol	Description	Value
R	The radius of the basin	200 m
v_{s1}	Shear wave velocity in the basin	500 m/s
v_{p1}	Compression wave velocity in the basin	1000 m/s
ρ_1	Density in the basin	2100 kg/m^3
η	Nondimensional frequency	0.5
ν_1, ν_2	Internal and external Poisson's ratio	1/3
v_{s2}	Shear wave velocity outside the basin	1000 m/s
v_{p2}	Compression wave velocity outside the basin	2000 m/s
ρ_2	Density outside the basin	1400 kg/m^3
ξ_1, ξ_2	Internal and external damping ratio	0.03

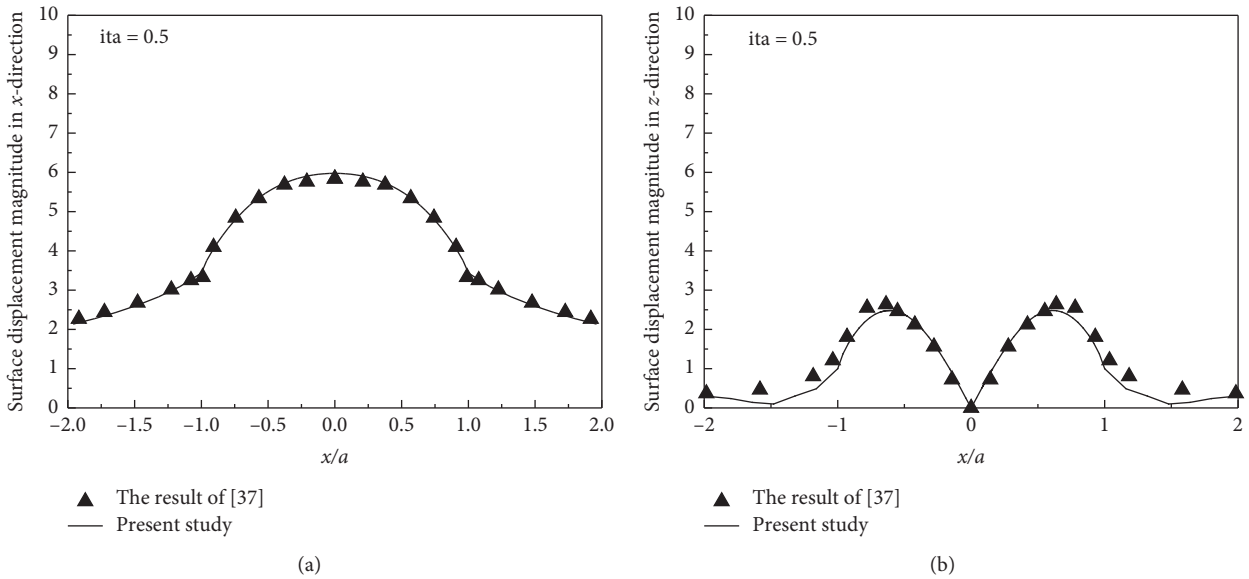

Figure 5: The displacement amplitude of surface node on x-axis of sedimentary basin: (a) the x-direction; (b) the z-direction.

Table 3: List of some important notations and values.

Symbol	Value
Basin parameters	
ν_1	0.3
ρ_1	2000 kg/m^3
ξ_1	0.03
v_{s1}	400 m/s
Out-of-basin parameter	
ν_2	0.25
ρ_2	2200 kg/m^3
ξ_2	0.02
v_{s2}	1000 m/s
Building parameters	
ν_c	0.18
ρ_c	2500 kg/m^3
ξ_c	0.05
E_c	3×10^7 Pa

buildings and no buildings and the position of the larger reaction area, the influence of the number of buildings on the seismic dynamic response of the homogeneous sedimentary basin is obtained.

Figures 6(a)–6(d)–11(a)–11(d) is the displacement reflection cloud image of the homogeneous sedimentary basin with the change of the number of buildings under the incidence of SV wave at different frequencies, and f is the frequency of the incident wave. Taking 6(a) as an example, the left side shows the x-direction displacement cloud map on the x-y plane of the homogeneous sedimentary basin, and the right side shows the x-direction displacement cloud map on the x-z plane and y-z plane of the homogeneous sedimentary basin from top to bottom.

As shown in Figure 6, at low frequency ($f = 0.5$ Hz), the presence of the basin has a strong "focusing effect" on the site, and the site at the center of the basin is very obvious, which makes the buildings located in the center of the sedimentary basin susceptible to great influence. For $f = 1$ Hz, the buildings act as a "secondary source" and produces a coherent effect with the scattered waves in the sedimentary basin, resulting in spatial redistribution of surface ground motion. With the increase of the number of buildings, the spatial position of the peak displacement gradually shifted from the surface point on the x-axis to the surface point on the y-axis, and the peak displacement position within the basin gradually moved to the center of the basin. At the same time, the existence of buildings will increase the displacement response of sedimentary basin. If there are no buildings in the basin, the peak displacement on the surface and inside of the basin are 5.5, as illustrated in Figure 7(a), and the peak displacement on the surface and inside of the basin are 6.8 and 7.4 (see Figure 7(d)) when the number of buildings 26×26, which increases by 23.6% and 34.5%, respectively.

Different from the 1 Hz case, when the frequency is 2 Hz, the buildings can effectively weaken the seismic response of the basin, the peak of displacement amplitude of no building reaches 7.9 (see Figure 8(a)), while the number of buildings is 26×26 and the basin displacement peaks is 5.1 (see Figure 8(d)), reducing 35.4%. Moreover, the buildings still has an obvious "focusing effect" on the scattered waves, and the peak displacement position in the basin is closer to the center of the basin as the number of buildings increases. Due to the coherent effect of the buildings on the waves, the peak displacement position in the x-direction of the whole basin shifted from near the surface to near the bottom of the basin.

Figure 9 shows the displacement reflection of the homogeneous sedimentary basin at the frequency is 3 Hz. The presence of the buildings reduces the peak displacement in the basin space, the peak of displacement amplitude of no building is 14.9 (see Figure 9(a)), while the number of buildings is 14×14 and the basin displacement peaks are 8.8 (see Figure 9(b)), reduced by 40.9%. However, the peak displacement in the x-direction moves from the basin

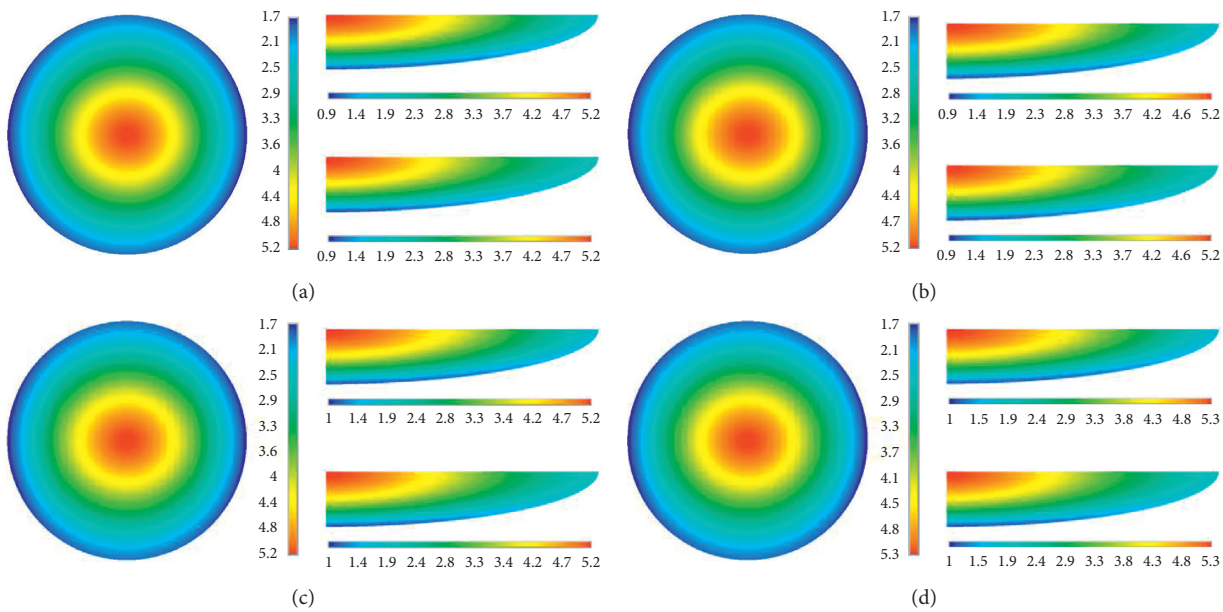

Figure 6: The displacement amplitude of the homogeneous sedimentary basin ($f = 0.5$ Hz): (a) no buildings; (b) buildings 14×14; (c) buildings 20×20; (d) buildings 26×26.

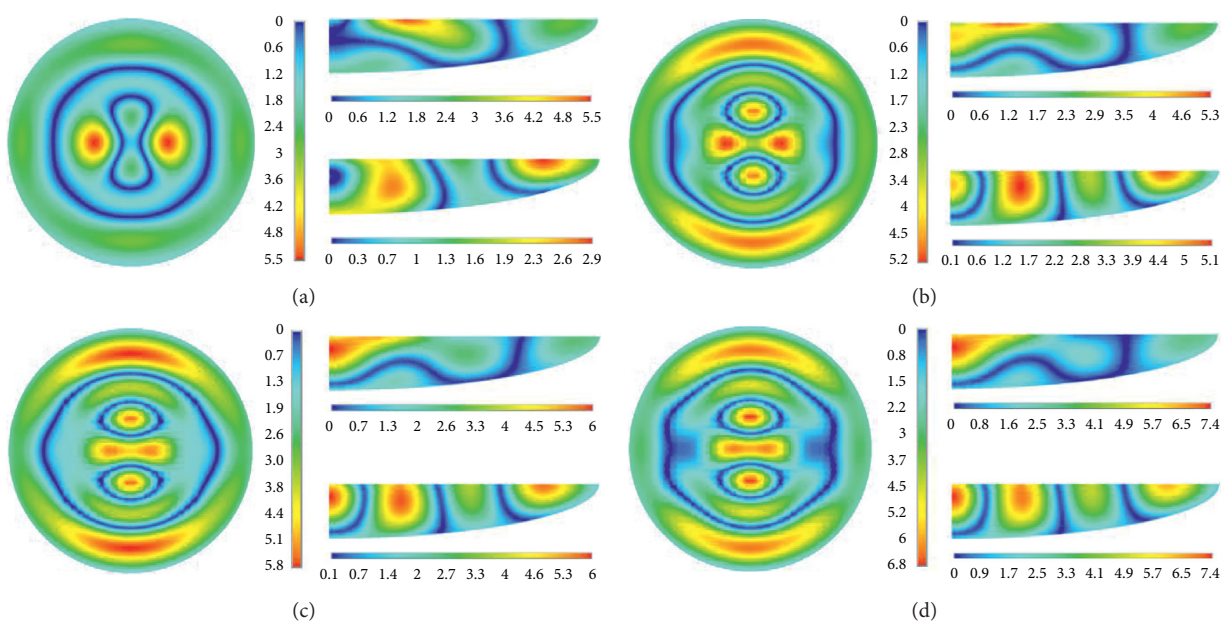

Figure 7: The displacement amplitude of the homogeneous sedimentary basin ($f = 1.0$ Hz): (a) no buildings; (b) buildings 14×14; (c) buildings 20×20; (d) buildings 26×26.

interior to the surface, resulting in a 57.4% increase in the x-direction displacement of the basin surface, as shown in Figures 9(a) and 9(d); the peak of displacement amplitude of no building is 6.8 and the number of buildings 26×26 is 10.7 because of the scattering effect of the buildings as a "secondary source" on the wave.

When the SV wave is incident at a frequency of 4 Hz, as illustrated in Figure 10, the "coherence effect" of buildings and homogeneous sedimentary basin is very obvious, and the existence of buildings will reduce the displacement response of homogeneous sedimentary basin and the displacement peak in the x-direction in the basin decreases with the increase of the number of buildings, such as the surface peak displacement of the no buildings' basin is 9.1 and the number of buildings 14×14, 20×20, and 26×26 are 8.7, 8.8, and 7.8, respectively. Figure 11 shows the case of the frequency 5 Hz; the buildings have the most significant weakening effect on the seismic response within the basin; when there were no buildings and the number of buildings 20×20, the peak displacement of the homogeneous sedimentary basin was 18.1 and 6.2, respectively, with a decrease of 65.7%. From the perspective of the whole basin, the

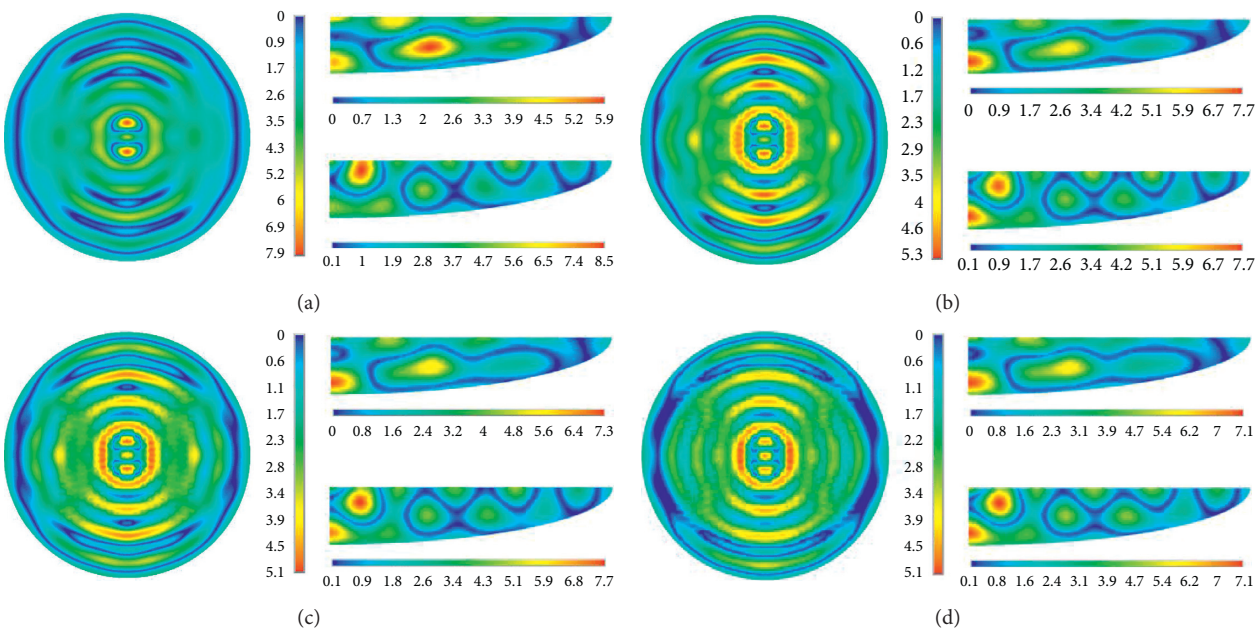

Figure 8: The displacement amplitude of the homogeneous sedimentary basin ($f = 2.0$ Hz): (a) no buildings; (b) buildings 14×14; (c) buildings 20×20; (d) buildings 26×26.

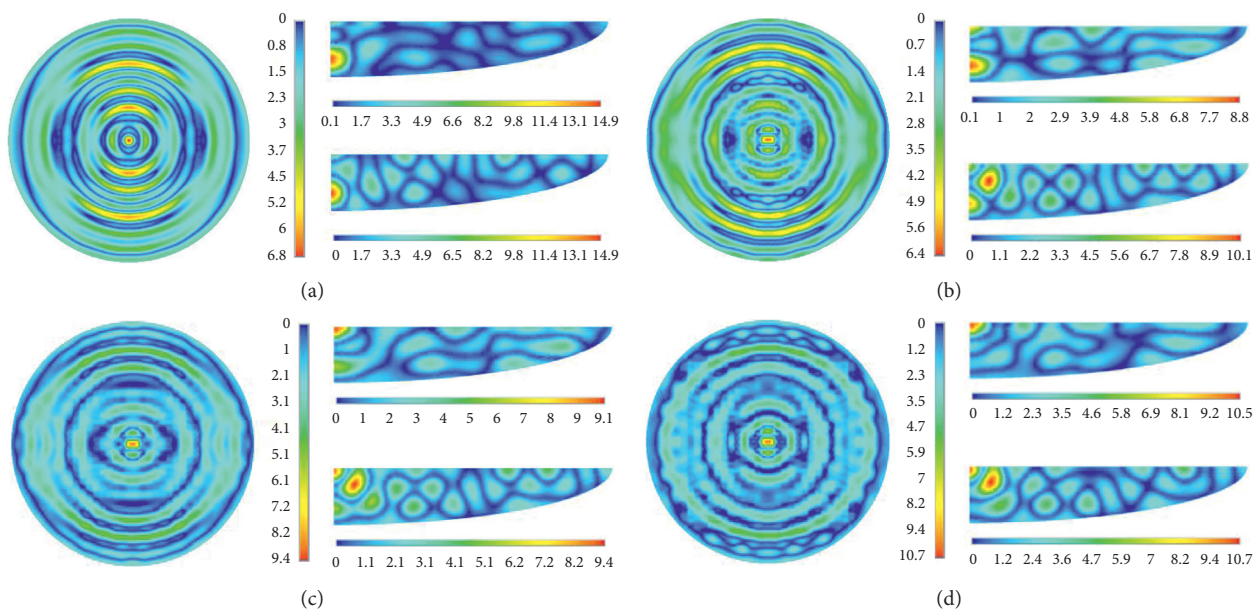

Figure 9: The displacement amplitude of the homogeneous sedimentary basin ($f = 3.0$ Hz): (a) no buildings; (b) buildings 14×14; (c) buildings 20×20; (d) buildings 26×26.

26×26 buildings has the best effect on the reduction of displacement amplitude in most areas of the basin space.

In general, at low frequency ($f = 0.5$ Hz), the "coherence effect" of the buildings on the scattered waves is not obvious, and the seismic response of the homogeneous basin is hardly affected. At a certain frequency ($f = 1$ Hz), the buildings will not only change the position of the peak displacement of the basin but also increase the peak displacement of the basin. At high frequency ($f \geq 2$ Hz), the existence of buildings weakens the seismic response of the homogeneous basin to different degrees, but the more the buildings, the better the weakening effect.

5.3. The Influence of Building Spacing on the Amplification Effect of Ground Motion in Homogeneous Sedimentary Basin. In order to explore the influence of building spacing on the homogeneous sedimentary basin under the action of earthquake, the displacement amplitude of the homogeneous sedimentary basin under different building spacing

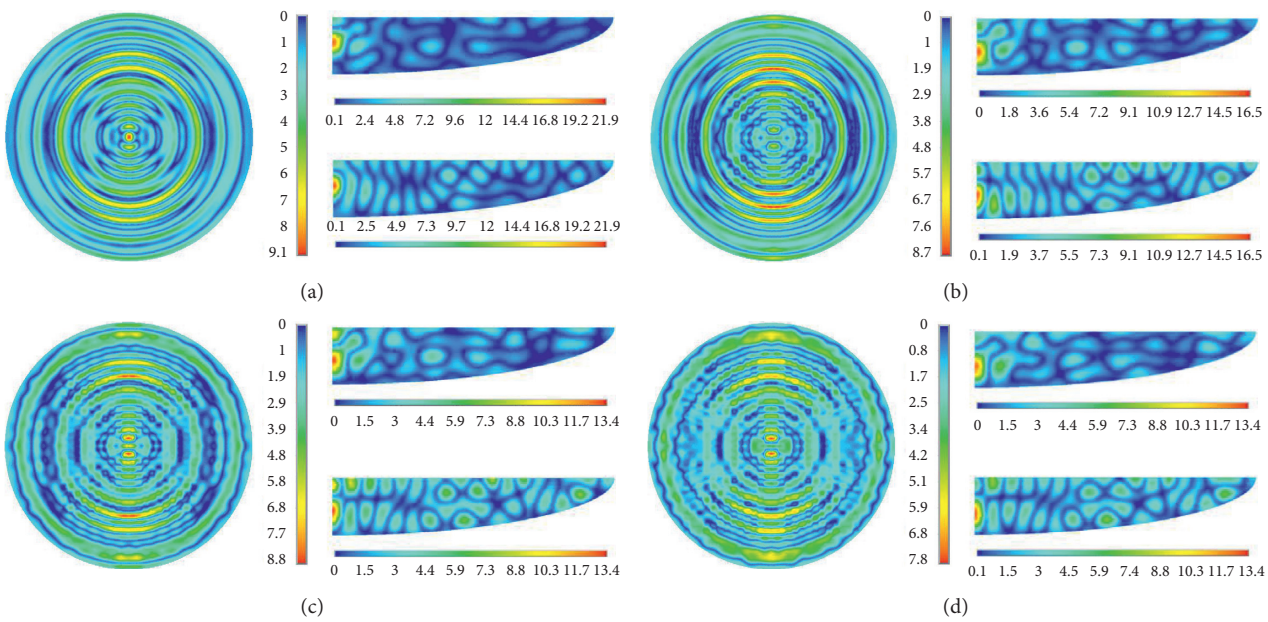

Figure 10: The displacement amplitude of the homogeneous sedimentary basin ($f = 4.0$ Hz): (a) no buildings; (b) buildings 14×14; (c) buildings 20×20; (d) buildings 26×26.

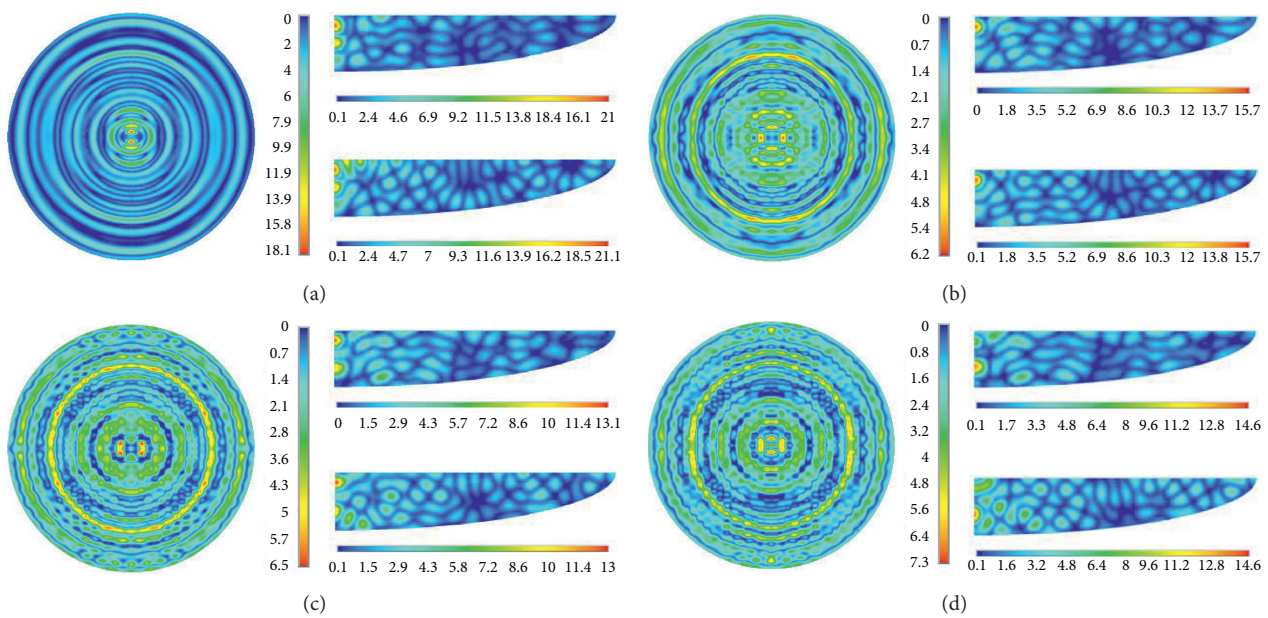

Figure 11: The displacement amplitude of the homogeneous sedimentary basin ($f = 5.0$ Hz): (a) no buildings; (b) buildings 14×14; (c) buildings 20×20; (d) buildings 26×26.

and no building was analyzed, as well as the location of the larger reaction area. In order to reduce unnecessary calculations, only 20×20 buildings are selected, and the seismic displacement response of homogeneous sedimentary basin under different building spacing is shown in Figures 12(a)–12(d)–17(a)–17(d).

When $f = 0.5$ Hz, as shown in Figure 12, in the case of different building spacing and no building, the homogeneous sedimentary basins all show obvious "focusing effect," which can make the buildings in the middle of the basin destroyed seriously. And the peak displacement in the x-direction of both the surface and the interior of the homogeneous basin is 5.2, indicating that the building spacing has no obvious influence on the seismic response of the homogeneous sedimentary basin at low-frequency incidence.

Figure 13 shows the displacement response of the basin with the different building spacing and no building at 1 Hz. It can be seen that the ground motion response of the surface of the basin will generate redistribution, changing from the

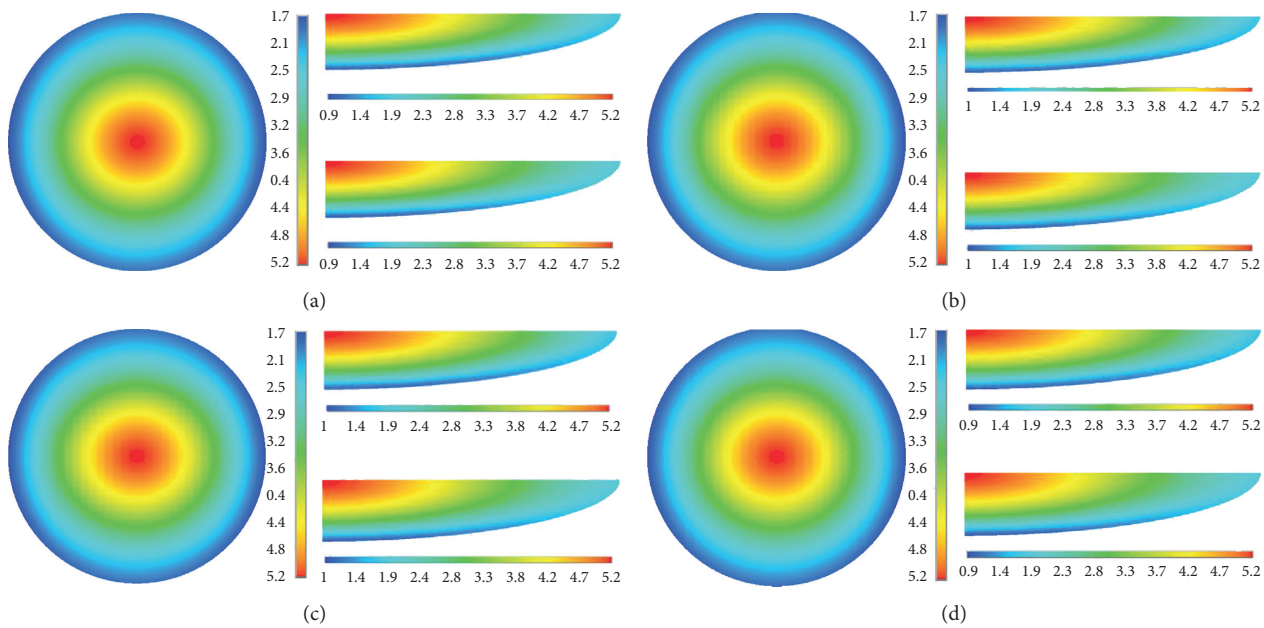

Figure 12: The displacement amplitude of the homogeneous sedimentary basin ($f = 0.5$ Hz): (a) no buildings; (b) $D = 55$ m; (c) $D = 62.5$ m; (d) $D = 70$ m.

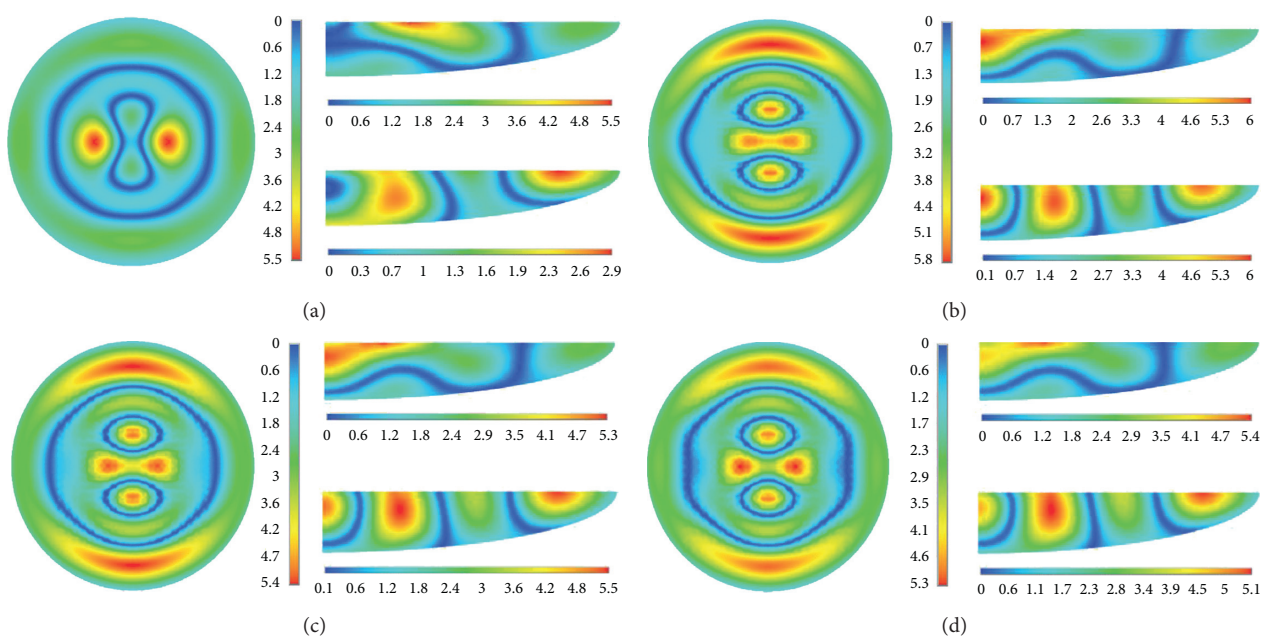

Figure 13: The displacement amplitude of the homogeneous sedimentary basin ($f = 1.0$ Hz): (a) no buildings; (b) $D = 55$ m; (c) $D = 62.5$ m; (d) $D = 70$ m.

"central focusing" of $f = 0.5$ Hz to the "multipoint focusing" along the y-axis, and the sites near $y/r = 2/5$ and $4/5$ of basin reflected very clearly and the buildings is easily affected. With the increase of building spacing, the displacement response of the basin gradually decreases. For example, in the case that the number of buildings is 20×20 and the building spacing $D = 55$ m, 62.5 m, and 70 m, the peak displacements of the basin are 5.8, 5.4, and 5.3, respectively. When $f = 2$ Hz, as shown in Figure 14, the buildings shows obvious characteristics of weakening the seismic response of the basin and with the increase of building spacing, the weakening effect of buildings becomes weaker, such as the surface peak displacement of the no buildings basin is 7.9, and the building spacing $D = 55$ m, 62.5 m and 70 m are 5.1, 6 and 6.3, decreased by 35.4%, 24.1% and 20.3% respectively.

When $f = 3$ Hz, the buildings also weakens the seismic response of the basin and the weakening effect is the best when the building spacing is 70 m, the peak displacement on

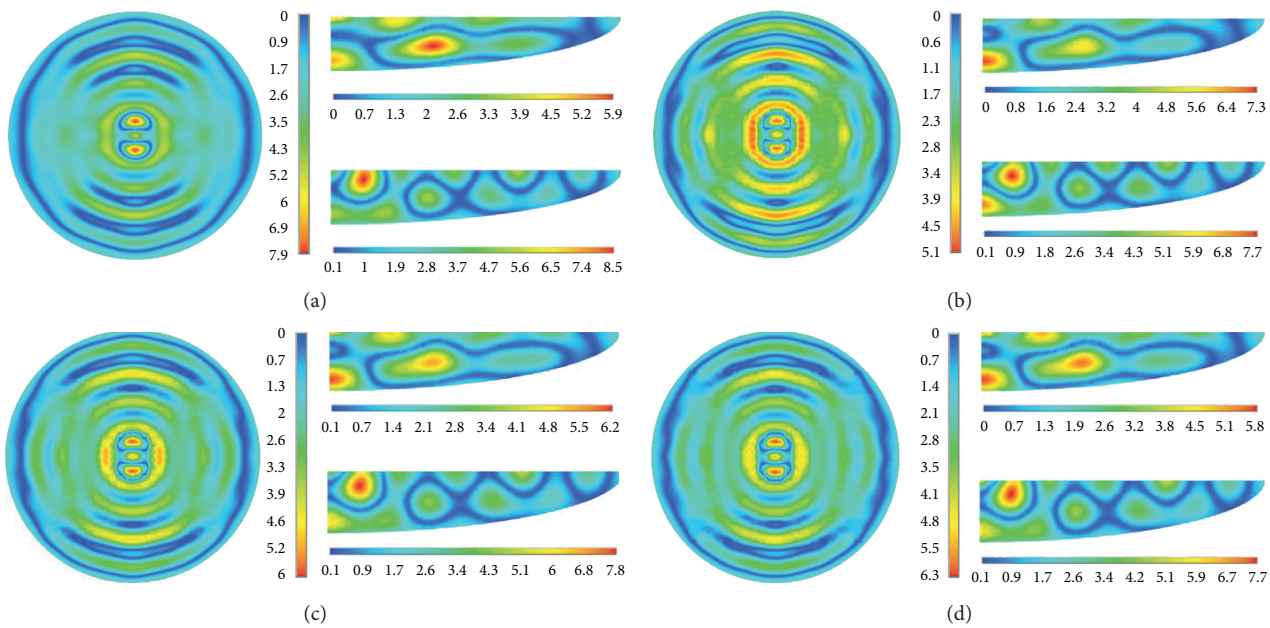

Figure 14: The displacement amplitude of the homogeneous sedimentary basin ($f = 2.0$ Hz): (a) no buildings; (b) $D = 55$ m; (c) $D = 62.5$ m; (d) $D = 70$ m.

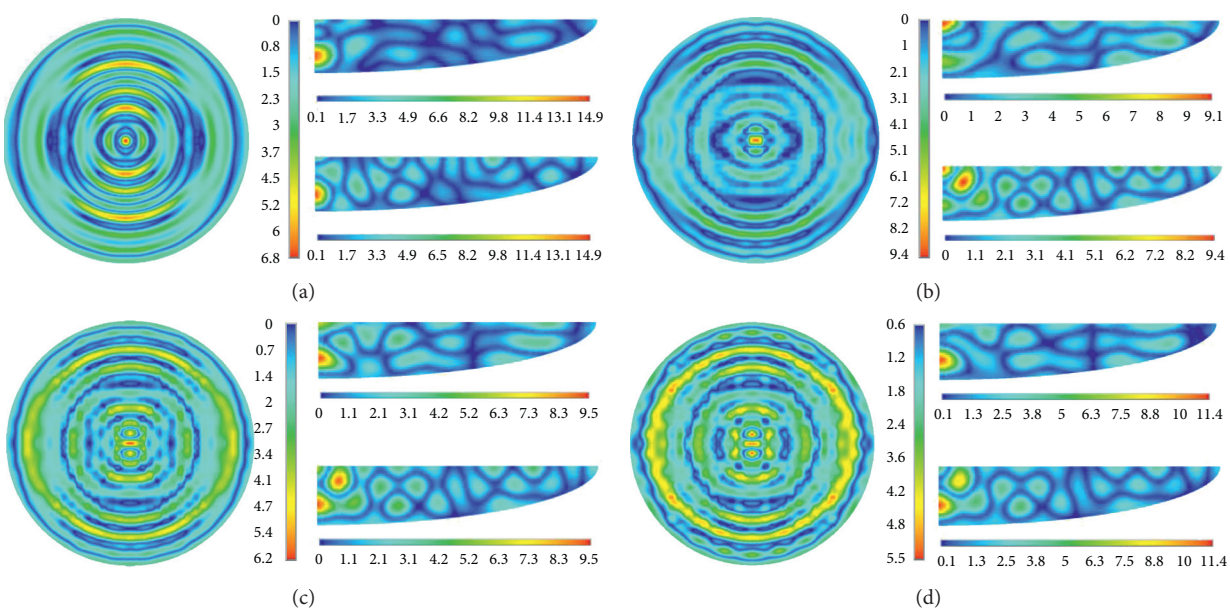

Figure 15: The displacement amplitude of the homogeneous sedimentary basin ($f = 3.0$ Hz): (a) no buildings; (b) $D = 55$ m; (c) $D = 62.5$ m; (d) $D = 70$ m.

the surface of the homogeneous basin in the x-direction of the no buildings is 6.8 (see Figure 15(a)), and that of $D = 70$ m is 5.5(see Figure 15(d)), decreased by 19.1%. However, when the building spacing is 55 m, the coherence effect of scattered waves in the basin is the strongest, and the peak displacements in the basin of the no buildings and the building when the spacing is 55 m are 6.8 and 9.4 (see Figures 15(a) and 15(b)), increased by 38.9%. At the same time, this also led to a more dramatic "focusing effect," which further magnified the peak displacement of the basin surface.

Figures 16 and 17 show the seismic displacement response of homogeneous sedimentary basin under different building spacings at 4 Hz and 5 Hz, respectively. The buildings significantly weakens the peak displacement in the homogeneous basin, and the smaller the building spacing, the more significant the weakening effect. For example, the displacement peaks of homogeneous sedimentary basins are 18.1 (see Figure 17(a)), 6.5 (see Figure 17(b)), and 6.9 (see Figure 17(c)), when there are no buildings, the building spacing is 55 m and the building spacing is 62.5 m, and the

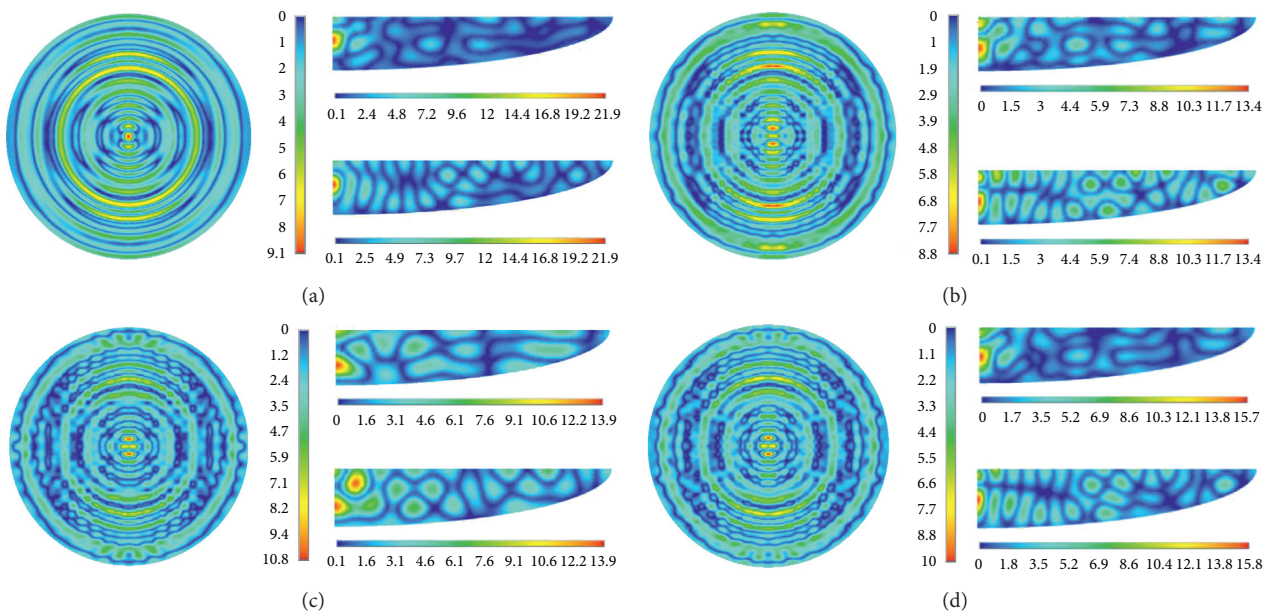

Figure 16: The displacement amplitude of the homogeneous sedimentary basin ($f = 4.0$ Hz): (a) no buildings; (b) $D = 55$ m; (c) $D = 62.5$ m; (d) $D = 70$ m.

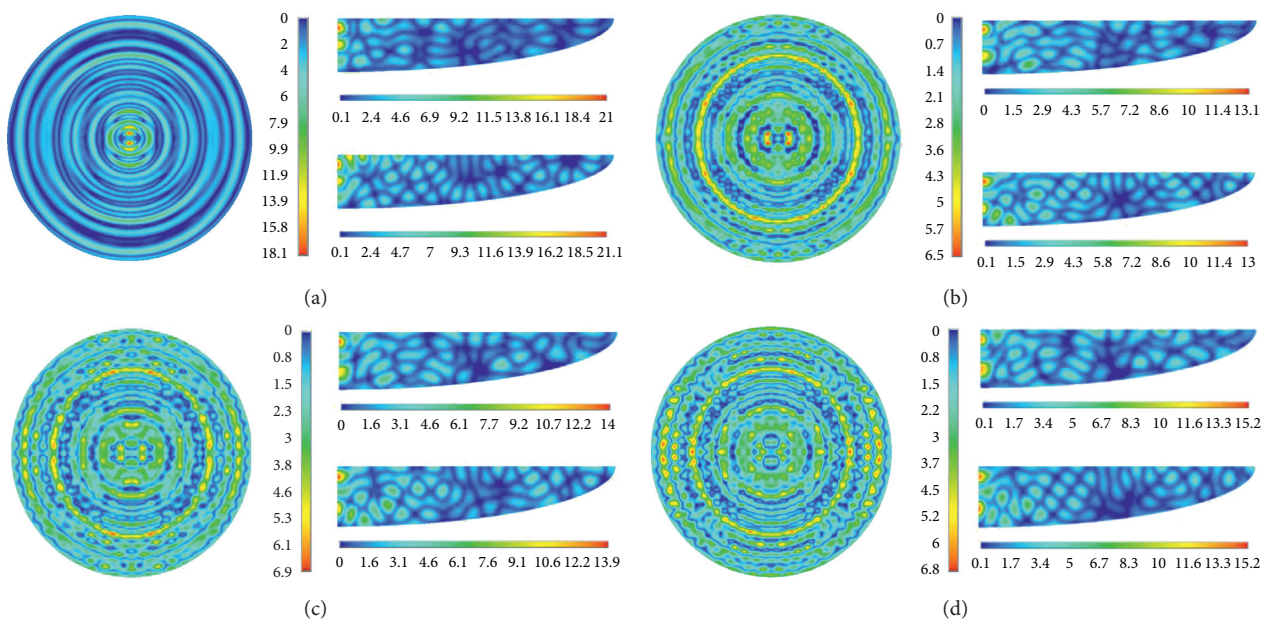

Figure 17: The displacement amplitude of the homogeneous sedimentary basin ($f = 5.0$ Hz): (a) no buildings; (b) $D = 55$ m; (c) $D = 62.5$ m; (d) $D = 70$ m.

seismic response of sedimentary basins is reduced by 64.1% and 61.9% due to the presence of buildings.

In summary, at low frequencies, the variation of building spacing has almost no effect on the peak displacement of homogeneous sedimentary basins. When the frequency is between 1 Hz and 3 Hz, the denser buildings will lead to the intensification of the "focusing effect" of the basin and the increase of the peak displacement in the basin. However, the existence of building groups can reduce the displacement amplitude of the whole basin.

6. Conclusions

In this paper, the harmonic response analysis module in the finite element simulation software ANSYS is used to carry out frequency domain analysis on the three-dimensional building group-homogeneous sedimentary basin model. The following conclusions are obtained:

(1) At low frequency ($f = 0.5$ Hz), the changes of the number of buildings and building spacing have little impact on the peak displacement in the x-direction

of the homogeneous sedimentary basin, and the displacement amplitude of basin shows the obvious phenomenon of "central focusing." So, it is necessary to avoid the central position as far as possible when building site selection in the basin.

(2) At a certain low frequency (1.0 Hz in this paper), as the buildings acts as a "secondary source" and generates a dramatic "coherence effect" with the scattered waves, the displacement response of the sedimentary basin is redistributed. The peak displacement of the basin moves to the center, and the position of the peak displacement of the surface also shifts from the node on the x-axis to the node on the y-axis.

(3) With the increase of frequency, the displacement amplitude of the homogeneous sedimentary basin changes from "central focusing" to "multipoint focusing," and the displacement peak gradually moves from the surface to the center of the basin. In addition, the peak displacement in the x-direction of the homogeneous sedimentary basin basically increases with the increase of incident wave frequency.

(4) The existence of buildings will weaken the seismic response of homogeneous sedimentary basin to different degrees. The larger the number of buildings, the smaller the space between buildings and the more significant the weakening effect of seismic response to homogeneous sedimentary basin.

Data Availability

The data used to support the findings of this study are available from the corresponding author upon request.

Conflicts of Interest

The authors declare that they have no conflicts of interest.

Acknowledgments

This study was financially supported by the National Natural Science Youth Fund of China (Grant no. 51608521).

References

[1] C. C. Mow and Y. H. Pao, *The Diffraction of Elastic Waves and Dynamic Stress Concentrations*, RAND Corporation, Santa Monica, California, 1971.

[2] T. Balendra, D. P. Thambiratnam, C. G. Koh, and S.-L. Lee, "Dynamic response of twin circular tunnels due to incident SH-waves," *Earthquake Engineering & Structural Dynamics*, vol. 12, no. 2, pp. 181–201, 1984.

[3] X. Yuan and Z. P. Liao, "Scattering of plane SH waves by a cylindrical canyon of circular-arc cross-section," *Soil Dynamics and Earthquake Engineering*, vol. 13, no. 6, pp. 407–412, 1994.

[4] X. M. Yuan, "Effect of a circular underground inclusion on surface motion under incident plane SH waves," *ACTA Geophysica Sinica*, vol. 39, no. 3, pp. 373–381, 1996.

[5] V. W. Lee, H. Luo, and J. Liang, "Antiplane (SH) waves diffraction by a semicircular cylindrical hill revisited: an improved analytic wave series solution," *Journal of Engineering Mechanics*, vol. 132, no. 10, pp. 1106–1114, 2006.

[6] R. Ávila-Carrera and F. J. Sánchez-Sesma, "Scattering and diffraction of elastic P-and S-waves by a spherical obstacle: a review of the classical solution," *Geofisica Internacional*, vol. 45, no. 1, pp. 3–21, 2006.

[7] X.-L. Zhou, L.-F. Jiang, and J.-H. Wang, "Scattering of plane wave by circular-arc alluvial valley in a poroelastic half-space," *Journal of Sound and Vibration*, vol. 318, no. 4-5, pp. 1024–1049, 2008.

[8] K. C. Wong, A. H. Shah, S. K. Datta, and K. D. Subhendu, "Dynamic stresses and displacements in a buried tunnel," *Journal of Engineering Mechanics*, vol. 111, no. 2, pp. 218–234, 1985.

[9] T. Toshinawa and T. Ohmachi, "Love-wave propagation in a three-dimensional sedimentary basin," *Bulletin of the Seismological Society of America*, vol. 82, no. 4, pp. 1661–1677, 1992.

[10] S. Turek, A. Obaid, and B. Markert, "On a fully implicit, monolithic finite element method-multigrid solution approach for dynamic porous media problems," *Journal of Coupled Systems and Multiscale Dynamics*, vol. 1, no. 2, pp. 224–240, 2013.

[11] H. Bao, J. Bielak, O. Ghattas et al., "Large-scale simulation of elastic wave propagation in heterogeneous media on parallel computers," *Computer Methods in Applied Mechanics and Engineering*, vol. 152, no. 1-2, pp. 85–102, 1998.

[12] N. Dai, A. Vafidis, and E. R. Kanasewich, "Wave propagation in heterogeneous, porous media: a velocity-stress, finite-difference method," *Geophysics*, vol. 60, no. 2, pp. 327–340, 1995.

[13] T.-S. Kang and C. E. Baag, "An efficient finite-difference method for simulating 3D seismic response of localized basin structures," *Bulletin of the Seismological Society of America*, vol. 94, no. 5, pp. 1690–1705, 2004.

[14] S.-J. Lee, H.-W. Chen, and B.-S. Huang, "Simulations of strong ground motion and 3D amplification effect in the Taipei basin by using a composite grid finite-difference method," *Bulletin of the Seismological Society of America*, vol. 98, no. 3, pp. 1229–1242, 2008.

[15] F. J. Sánchez-Sesma and M. Campillo, "Diffraction of P, SV, and Rayleigh waves by topographic features: a boundary integral formulation," *Bulletin of the Seismological Society of America*, vol. 81, no. 6, pp. 2234–2253, 1991.

[16] M. Vinski and T. K. Mossessian, "Scattering of plane harmonic P, SV, and Rayleigh waves by dipping layers of arbitrary shape," *Bulletin of the Seismological Society of America*, vol. 77, no. 1, pp. 212–235, 1987.

[17] F. Luzón, F. J. Sánchez-Sesma, J. A. Pérez-Ruiz, L. Ramírez-Guzmán, and A. Pech, "In-plane seismic response of inhomogeneous alluvial valleys with vertical gradients of velocities and constant Poisson ratio," *Soil Dynamics and Earthquake Engineering*, vol. 29, no. 6, pp. 994–1004, 2009.

[18] H. Kawase and K. Aki, "A study on the response of a soft basin for incident S, P, and Rayleigh waves with special reference to the long duration observed in Mexico City," *Bulletin of the Seismological Society of America*, vol. 79, no. 5, pp. 1361–1382, 1989.

[19] T. K. Mossessian and M. Dravinski, "Application of a hybrid method for scattering of P, SV, and Rayleigh waves by near-surface irregularities," *Bulletin of the Seismological Society of America*, vol. 77, no. 5, pp. 1784–1803, 1987.

[20] Z. X. Liu and D. Wang, "Effect of different wave velocity models on seismic response of alluvial valley based on FEM-

IBIEM," *Chinese Journal of Geotechnical Engineering*, vol. 36, no. 7, pp. 1289–1301, 2014.

[21] J. G. Anderson, P. Bodin, J. N. Brune et al., "Strong ground motion from the michoacan, Mexico, earthquake," *Science*, vol. 233, no. 4768, pp. 1043–1049, 1986.

[22] P. Arben and I. Kojiro, "Basin structure effects on long-period strong motions in the san fernando valley and the los Angeles basin from the 1994 northridge earthquake," *Bulletin of the Seismological Society of America*, vol. 86, no. 1, pp. 126–137, 1996.

[23] Y. B. Tsai and M. W. Huang, *Strong Ground Motion Characteristics of the Chichi, Taiwan, Earthquake of September 21, 1999*, Institute of Geophysics, National Central University, Taoyuan City, Taiwan, 2000.

[24] M. D. Trifunac, "Scattering of plane SH wave by a semi-cylindrical canyon," *Earthquake Engineering and Structural Dynamics*, vol. 1, no. 3, pp. 267–281, 1973.

[25] V. W. Lee, "Three-dimensional diffraction of plane P, SV & SH waves by a hemispherical alluvial valley," *International Journal of Soil Dynamics and Earthquake Engineering*, vol. 3, no. 3, pp. 133–144, 1984.

[26] P. Li, H. S. Liu, and J. S. Bo, "Effects of river valley topography on anomalously high intensity in the Hanyuan town during the Wenchuan MS8.0 earthquake," *Chinese Journal of Geophysics*, vol. 59, no. 1, pp. 174–184, 2016.

[27] A. Wirgin and P.-Y. Bard, "Effects of buildings on the duration and amplitude of ground motion in Mexico City," *Bulletin of the Seismological Society of America*, vol. 86, pp. 914–920, 1996.

[28] D. Clouteau and D. Aubry, "Modifications of the ground motion in dense urban areas," *Journal of Computational Acoustics*, vol. 9, no. 4, pp. 1659–1675, 2001.

[29] C. Tsogka and A. Wirgin, "Simulation of seismic response in an idealized city," *Soil Dynamics and Earthquake Engineering*, vol. 23, no. 5, pp. 391–402, 2003.

[30] M. Kham, J.-F. Semblat, P.-Y. Bard, and P. Dangla, "Seismic site-city interaction: main governing phenomena through simplified numerical models," *Bulletin of the Seismological Society of America*, vol. 96, no. 5, pp. 1934–1951, 2006.

[31] R. Taborda and J. Bielak, "Full 3D integration of site-city effects in regional scale earthquake simulations," in *Proceedings of the 8th International Conference on Structural Dynamics, EURODYN*, pp. 511–518, Leuven, Belgium, 2011.

[32] D. Volkov and S. Zheltukhin, "Preferred frequencies for coupling of seismic waves and vibrating tall buildings," *Soil Dynamics and Earthquake Engineering*, vol. 74, pp. 25–39, 2015.

[33] C. R. He, L. Yan, and Z. X. Liu, "Influence of urban intensive building groups on the ground motion amplification effect of an alluvial valley," *China Earthquake Engineering Journal*, vol. 41, no. 4, pp. 1035–1045, 2019.

[34] J. Liu, Y. Du, X. Du, Z. Wang, and J. Wu, "3D viscous-spring artificial boundary in time domain," *Earthquake Engineering and Engineering Vibration*, vol. 5, no. 1, pp. 93–102, 2006.

[35] M. H. Bazyar and C. Song, "A continued-fraction-based high-order transmitting boundary for wave propagation in unbounded domains of arbitrary geometry," *International Journal for Numerical Methods in Engineering*, vol. 74, no. 2, pp. 209–237, 2008.

[36] J. B. Liu, Y. Gu, and Y. X. Du, "Consistent viscous-spring artificial boundaries and viscous-spring boundary elements," *Chinese Journal of Geotechnical Engineerin*, vol. 28, no. 9, pp. 1070–1075, 2006.

[37] T. K. Mossessian and M. Dravinski, "Amplification of elastic waves by a three dimensional valley. Part 1: steady state response," *Earthquake Engineering & Structural Dynamics*, vol. 19, no. 5, pp. 667–680, 1990.